Biogeochemistry
https://doi.org/10.1007/s10533-022-00999-5

Carbon dynamics and greenhouse gas outgassing in an estuarine mangrove wetland with high input of riverine nitrogen

Zeyang Lu · Fenfang Wang · Kai Xiao · Yao Wang · Qibiao Yu · Peng Cheng · Nengwang Chen

Received: 23 July 2022 / Accepted: 18 November 2022

Abstract The large amounts of organic carbon buried in mangrove wetlands are well recognized, but the lateral dissolved carbon export and greenhouse gas (GHGs) outgassing are often overlooked. In this study, we carried out seasonal observations of dissolved carbon and GHGs in an estuarine mangrove wetland with high input of riverine nitrogen in southeast China in 2019–2020. The results showed that the tidal range and season were the two main factors controlling the lateral dissolved carbon export including total alkalinity (TA), dissolved inorganic carbon (DIC) and dissolved organic carbon (DOC). The positive correlations between the average offsets of DIC, TA, DOC and tidal range confirmed the hydrological controls on the exchange of dissolved carbon between the mangrove creek and the estuary. The seasonal variability in temperature, groundwater export and freshwater input resulted in a larger carbon offset during low tidal range in spring and a smaller offset during high tidal range in fall. The mangrove creek acted as a net source of DIC, DOC, TA and GHGs. When the emissions of GHGs were calculated as CO_2-equivalents, the average emission of CO_2 was four times higher than that of N_2O and the average emission of N_2O was six times higher than that of CH_4. In contrast with pristine mangroves, denitrification in mangrove wetlands with high input of riverine nitrogen played a crucial role in mineralization processes, leading to the production of DIC, TA and N_2O. These biogeochemical processes may not be conducive to the blue carbon sequestration in mangrove soils. These findings suggested that there are mutual benefits between the reduced loss of blue carbon and the mitigation of eutrophication when restoring mangrove wetlands and reducing nitrogen pollution.

Keywords Coastal wetlands · Blue carbon · Denitrification · CO_2-equivalent · Zhangjiang estuary

Responsible editor: Scott Neubauer.

Supplementary Information The online version contains supplementary material available at https://doi.org/10.1007/s10533-022-00999-5.

Z. Lu · F. Wang · Y. Wang · Q. Yu · N. Chen (✉)
Key Laboratory of the Coastal and Wetland Ecosystems, College of the Environment and Ecology, Xiamen University, Xiamen, China
e-mail: nwchen@xmu.edu.cn

Z. Lu · F. Wang · Y. Wang · Q. Yu · P. Cheng · N. Chen
State Key Laboratory of Marine Environment Science, Xiamen University, Xiamen, China

K. Xiao
State Environmental Protection Key Laboratory of Integrated Surface Water-Groundwater Pollution Control, School of Environmental Science and Engineering, Southern University of Science and Technology, Shenzhen, China

N. Chen
National Observation and Research Station for the Taiwan Strait Marine Ecosystem (Xiamen University), Zhangzhou, China

Published online: 09 December 2022

Introduction

Mangrove, together with seagrass and salt marshes, are important blue carbon ecosystems. They have important roles in the carbon cycle in coastal habitats and have a higher capacity to store carbon than land forest ecosystems (Donato et al. 2011). Most of the research on the carbon cycle in blue carbon habitats has focused on quantification of the storage and burial rate of soil carbon (Atwood et al. 2017; Breithaupt et al. 2012; Donato et al. 2011; Sanders et al. 2016). The carbon burial potential in mangroves is correlated with the primary productivity of plants, the capture of sediment particles, the fluvial input of organic carbon and the anaerobic environment of sediments (Kelleway et al. 2016). However, many studies have shown that the lateral outwelling rates of dissolved inorganic carbon (DIC, where $DIC = CO_2 + HCO_3^- + CO_3^{2-}$) are higher than the rate of burial of carbon (Maher et al. 2018; Santos et al. 2019). Some of the buried carbon is mineralized and exported laterally to adjacent waters in the forms of dissolved carbon and dissolved greenhouse gases (GHGs) (Reithmaier et al. 2020). Comprehensive studies of the lateral export of DIC and dissolved organic carbon (DOC) and the emission of GHGs from mangrove tidal creeks are still scarce.

Previous studies have shown that the carbon sink in the global mangrove carbon budget has been underestimated by 50% (Adam 2011; Bouillon et al. 2007). This underestimation is related to water–air fluxes of CO_2 and the lateral export of carbon driven by porewater exchange (Alongi 2020a; Lovelock et al. 2014; Maher et al. 2013). It is therefore essential to explore the lateral export of carbon and the emission of GHGs at the water–air interface in mangrove wetlands. The submarine discharge of groundwater can be defined as the seepage of fresh groundwater and recirculated seawater into the tidal creek through a sand bed or coastal aquifer (Taniguchi et al. 2002). During an ebb tide, tidal creeks are enriched with DIC and DOC originating from surface and subsurface runoff, sediment resuspension and groundwater/porewater discharge (Taillardat et al. 2018). Seawater circulation is assumed to account for a substantial proportion of the missing carbon sink of mangroves (Bouillon et al. 2008). Several physical parameters influence the transfer of carbon from mangroves to tidal creeks, including the topography, sediment permeability, crab burrows and tidal pumping (Mazda and Ikeda 2006; Tait et al. 2016). Tidal pumping was a physical process driving seawater recirculation into coastal sediments. In brief, seawater infiltrates into sediment at flood tides, mixed with groundwater, and was discharged at ebb tides. Besides, the hydraulic gradient formed during the ebb tide will drive the groundwater discharge (Santos et al. 2012). However, the effects of tidal range and seasonal variability on the lateral carbon export have rarely been studied.

The emission of GHGs at the water–air interface is one of the pathways by which carbon is lost from mangrove wetlands and can offset carbon capture and storage in this habitat (Bouillon et al. 2008; Call et al. 2015; Santos et al. 2019). CH_4 and N_2O are powerful GHGs affecting the Earth's climate, with global warming potentials 27 and 273 times larger, respectively, than that of CO_2 for a 100-year period (IPCC 2021). However, synchronous measurements of the fluxes of CO_2, CH_4 and N_2O and a comparison of their CO_2-equivalent greenhouse gas flux in coastal wetlands have rarely been reported. Organic carbon cannot be permanently stored in wetland sediments as a result of the microbial activity that regulates the complex mineralization processes and promotes the production of CO_2 and CH_4 (Luo et al. 2019). Nitrification and denitrification are the main processes for the production of N_2O (Cole and Caraco 2001). GHGs produced in sediments enter the tidal creek with porewaters. The production of GHGs is related to the temperature, dissolved oxygen (DO) status, microbiological composition and sediment properties (e.g., salinity and pH) (Livesley and Andrusiak 2012). The concentration and emission fluxes of GHGs have a high spatiotemporal variability, but limited data are available (Linto et al. 2014). It is therefore imperative to study the fluxes of GHGs at the water–air interface in different seasons.

In this study, we focused on the lateral dissolved carbon export and GHGs emissions in an estuarine mangrove wetland with high input of riverine nitrogen in the Yunxiao National Mangrove Reserve, Fujian province, China. We conducted four time series of observations of dissolved carbon (DIC, DOC), the total alkalinity (TA) and GHG emissions (CO_2, CH_4 and N_2O) and longitudinal surveys of the tidal creek–estuary during 2019–2020. The specific objectives of this study were to: (1) evaluate the lateral export of carbon from the mangrove

tidal creek to the estuary in different seasons and under different tidal ranges; (2) explore the flux of GHGs and compare their greenhouse effect at the water–gas interface in different seasons; and (3) reveal the major biogeochemical processes driving the production of alkalinity and DIC in mangrove sediments.

Materials and methods

Study site

Field investigations were performed at Yunxiao National Mangrove Reserve and Zhangjiang estuary in southeast China, a typical subtropical tidal estuary (Fig. 1). The mangroves of the tidal creek are

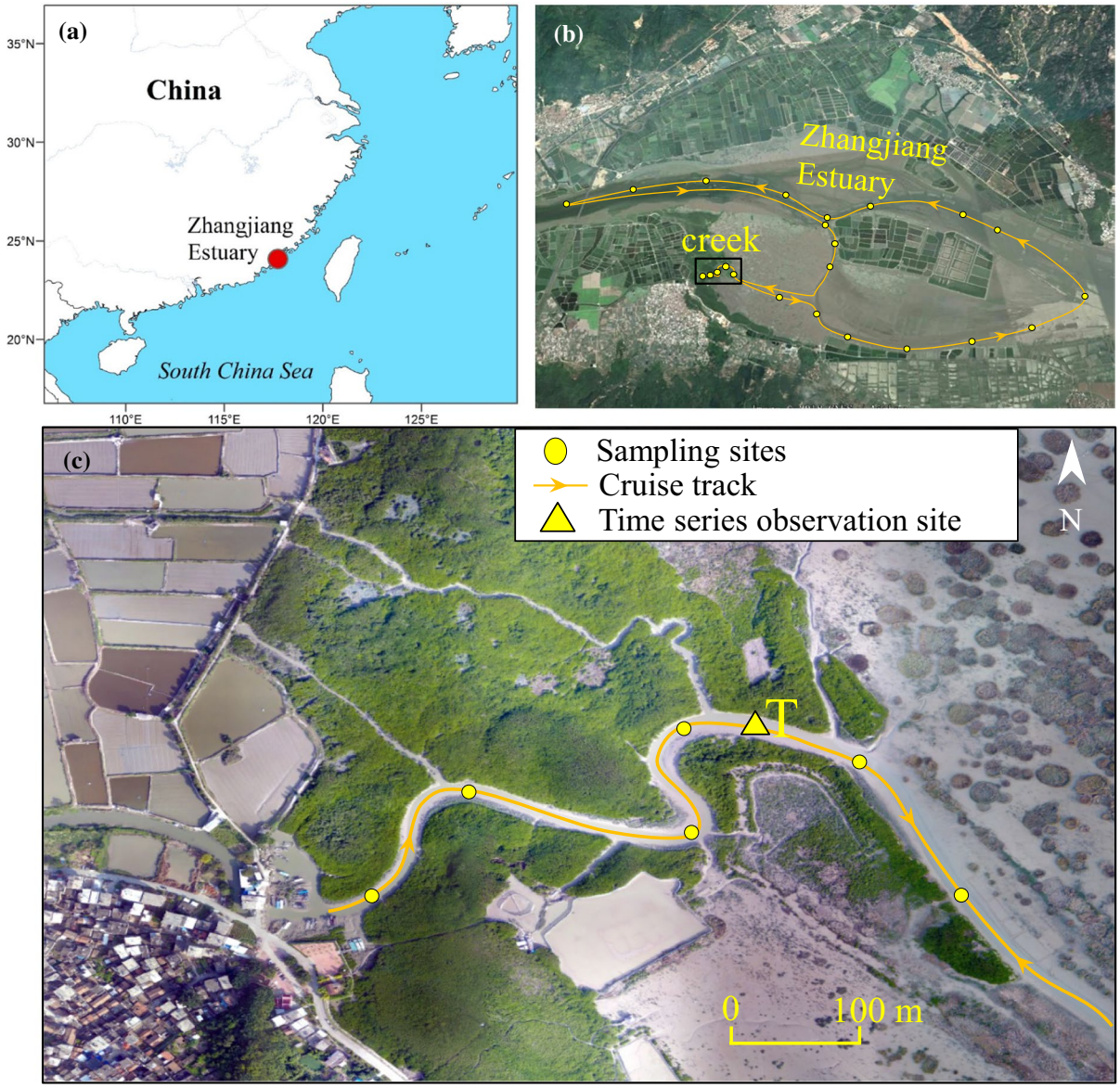

Fig. 1 Map of study areas showing sampling sites along Zhangjiang Estuary (**b**) and a main tidal creek (**c**) in Yunxiao National Mangrove Reserve, Fujian Province, China. The arrows on the line indicate cruise track direction. Time series measurements (site T) were performed at the outlet of the mangrove forest catchment. Modified after Wang et al. (2019)

dominated by *Avicennia marina*, *Kandelia candel* and *Aegiceras corniculatum* (Zhou et al. 2010). The climate in this area is subtropical with an annual precipitation of 1680 mm and seasonal mean temperatures ranging from 15.9 to 28.8 °C. There is an irregular semidiurnal tide with a tidal range of 0.43–4.67 m (Zhang et al. 2006). This means that there is a high tidal range and a low tidal range in the day's tidal cycle (Fig. 3). During low tide, effluents from upstream flow into the mangrove creek via dikes with sluices (Wang et al. 2010). The estuarine water has a high concentration of nitrate (> 140 μmol L^{-1}) and flows into the mangrove wetland during flood tides (Wang et al. 2019).

Sample collection and analysis

Four cruises were conducted to explore the seasonal and tidal range variation in carbon exports: November 15–17, 2019 (fall), December 17–19, 2019 (winter), May 27–29, 2020 (spring) and August 17–19, 2020 (summer). During each cruise, surface water samples were collected from the tidal creek in the mangrove to the estuary. In the tidal creek, we collected samples during both ebb and flood tide to compare the concentration of dissolved carbon in mangrove zone and estuarine water. In addition, a 25-h time series of fixed-site (station T) measurements were conducted to study the effect of tides and the season on carbon export and the emission of GHGs. Station T was located at the outlet of the tidal creek of mangrove forest. Seepage water samples were collected on the slope of the tidal creek at low tide.

Salinity, water temperature, DO and pH were measured in situ using a multi-parameter portable meter (Multi 3430, Germany). The water depth was measured using a sonar sonde (SM-5A, USA). Surface (0.5 m) water samples were collected using a Niskin hydrophore. The DIC, TA and greenhouse gas (CH_4 and N_2O) samples were collected in 40-mL brown glass vials, 125-mL high-density polyvinyl chloride bottles and 60-mL brown glass vials, respectively, all without any headspace or bubbles. After treating on collection with 0.1% saturated $HgCl_2$, the samples were analyzed within one week.

To determine the DOC, the water samples were filtered through 0.7-μm pre-combusted (500 °C for 10 h) GF/F filters. The filtrates were acidified and stored at 4 °C. The concentrations of DIC were measured using a CO_2/H_2O analyzer (LI 7000). A classic Gran titration method with an automated titrator was used to measure TA. The DIC and TA were calibrated against a certified reference material from A. Dickson of the Scripps Institution of Oceanography (San Diego, CA, USA) (see details in Cai et al. 2004). Both DIC and TA samples were tested for three times to reduce the uncertainty. The precision from repeated analysis was ± 2 μmol kg^{-1}. DOC was determined using a TOC-V CPH total organic carbon analyzer (Shimadzu, Japan) according to Wu et al. (2015). Deep seawater and low carbon reference waters (Hansell Laboratory, University of Miami, FL, USA) were used for quality control during sample analysis. The coefficient of variation of replicate measurements was < 2%. The partial pressure of the CO_2 (pCO_2) samples was calculated based on the measured TA and DIC using the CO_2SYS program (Lewis et al. 1998). Gas samples for the analysis of dissolved CH_4 and N_2O were obtained using a headspace method (Cotovicz et al. 2016). N_2 was injected into full bottles of samples to replace the water and the samples were shaken vigorously to obtain complete equilibrium between the water and air phases. The concentrations of CH_4 and N_2O were determined by gas chromatography (Agilent 7890A, USA) (Barnes et al. 2006).

Water–air GHGs flux

The water–air GHGs flux was calculated by:

$$F = k\alpha\left(C_{\mathrm{w}} - C_{\mathrm{air}}\right) \quad (1)$$

where F is the water–air flux (mmol m^{-2} h^{-1}), k is the gas transfer velocity (m h^{-1}), α is the solubility coefficient of the GHGs at a specific temperature and salinity, C_{w} is the concentration of GHGs in the water and C_{air} is the concentration of GHGs in the atmosphere. The solubility coefficients for CO_2, N_2O and CH_4 were determined according to Weiss (1974) and Yamamoto et al. (1976). The atmospheric values were assumed to be constant at 412 ppm for CO_2, 1.8 ppm for CH_4 and 0.33 ppm for N_2O (Reithmaier et al. 2020). The five models used to calculate the k values were:

$$k = 2.15 + 0.35v \quad (2)$$

$$k = 0.11 + 0.32v + 0.79u \quad (3)$$

$$k = -0.08 + 0.26v + 0.83u + 0.59h \quad (4)$$

$$k = 0.77v^{0.5}h^{-0.5} + 0.266u^2 \quad (5)$$

$$k = 1.0 + 1.719v^{0.5}h^{-0.5} + 2.58u \quad (6)$$

where v is the current velocity, u is the wind speed and h is the water depth. The hourly water speed was calculated using the primitive equation unstructured grid Finite Volume Community Ocean Model (FVCOM) (Chen et al. 2006). The model was validated with the tidal elevation data measured at Dongshan Bay (Fig. S1) and station T in the tidal creek. The details of model are given in the Supplementary Information. The wind speed was measured at a flux tower near the fixed station T. Equations 2, 3 and 4 were determined using a floating chamber in similar mangrove systems (Rosentreter et al. 2017) (R17). Equation 5 (Ho et al. 2016) (H16) and Eq. 6 (Borges et al. 2004) (B04) are commonly used in estuaries. To compare the fluxes of GHGs, the CH_4 and N_2O fluxes were converted into CO_2-equivalents using global warming potential ratio values of 273 and 27 (1 g of CH_4 = 27 g of CO_2; 1 g of N_2O = 273 g of CO_2) for emission time frames of 100 years (IPCC 2021).

Statistical analysis

One-way analysis of variance (ANOVA) was used to test the seasonal variability and relationships among parameters, including the water temperature, salinity, pH, DO, dissolved carbon and concentrations of GHGs. The significance level was set at $p < 0.05$. The water level data below 0.8 m were not included in the statistical analysis due to the impact of sewage discharge at the lowest tide. SPSS19.0 software was used to perform the statistical analysis.

Results

Spatial surveys

The trends of all the measured parameters (DIC/TA/DOC) were consistent throughout the four seasons of the spatial surveys (Fig. 2). The concentrations of DIC and TA in the estuary increased with increasing salinity, whereas the concentrations of DOC decreased. As the rainy season approached, the salinity of the surface water in the estuary gradually decreased and was lowest in summer. DIC, TA and DOC all showed conservative behavior in the Zhangjiang estuary. For a given salinity, the DIC, TA and DOC in the tidal creek were always higher than those in the estuary during the ebb tide (Fig. 2). There were significant positive correlations between the tidal range and the average offset of DIC ($R^2 = 0.92$, $p < 0.001$), TA ($R^2 = 0.76$, $p < 0.001$) and DOC ($R^2 = 0.91$, $p < 0.001$) during the ebb tide, with the exception of the low tide range cycle in spring and the high tide range cycle in the fall (where the offset is the deviation of the concentration from the regression line of the estuarine data points) (Fig. 4).

Variabilities in the timescales of tides and seasons

The surface water dynamics in the mangrove tidal creek were revealed in the four series of observations. The salinity, pH and DO varied greatly throughout the time series. These parameters followed the tidal variation, increasing during the flood tide and decreasing during the ebb tide (Fig. 3) and there were clear seasonal differences in salinity and temperature (Table 1). The temperature was significantly higher in spring and summer than in fall and winter, whereas the salinity was lower in spring and summer than in fall and winter.

The salinity, pH and DO did not follow a strict tidal cycle under the influence of sewage discharge at low tide. DIC, DOC, pCO_2, CH_4 and N_2O had a negative relationship with the water level, with higher values during ebb tides and lower values during flood tides (Fig. 3). pCO_2 showed significant seasonal variations, varying from 1191 to 4027 µatm during the wet seasons (summer and spring) and from 928 to 2574 µatm during the dry seasons (fall and winter) (Table 1). The concentrations of dissolved CH_4 and N_2O did not show significant seasonal variations. The DIC, TA, DOC and GHGs concentrations in the seepage water were significantly higher than those in the surface waters of the tidal creek (Table 1).

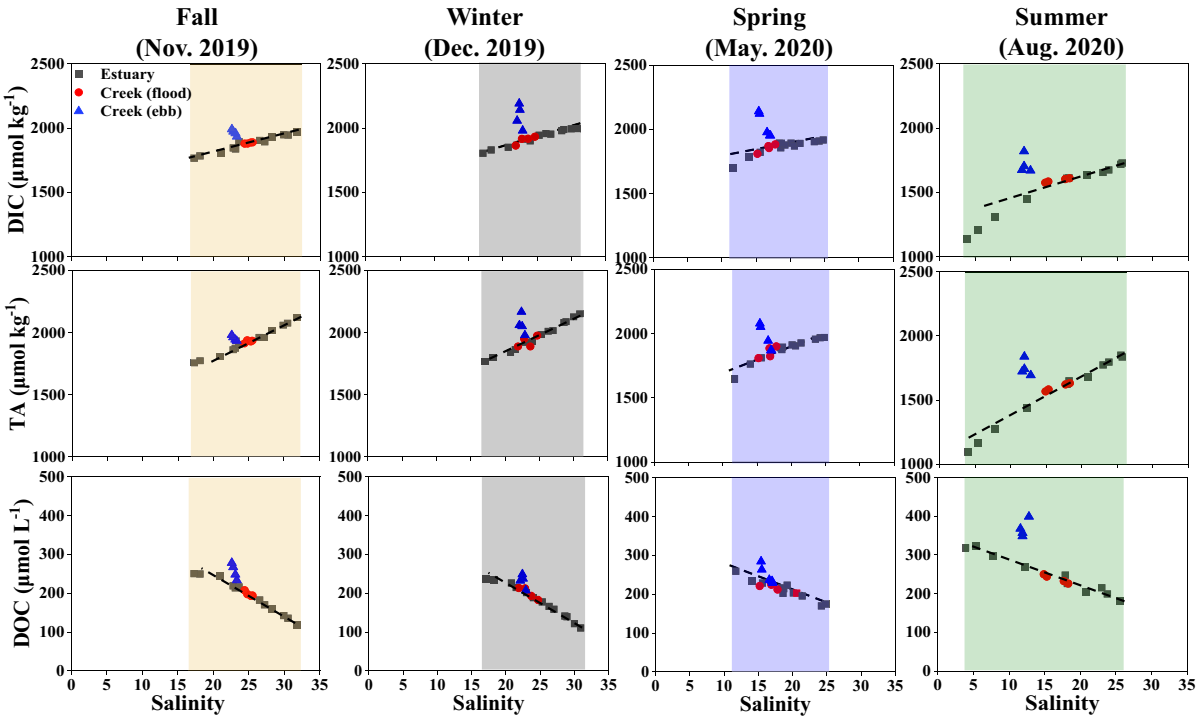

Fig. 2 The linear relationship between measured DIC, TA, DOC and salinity from Nov. 2019–Aug. 2020. Circles and triangles indicate the creek water samples during flood and ebb tide, respectively. The dotted regression lines indicated conservative mixing along the higher salinity gradient

GHGs fluxes at the water–air interface

The outgassing fluxes of GHGs were estimated using three different gas transfer velocity models to illustrate the possible ranges (Table S1). The average outgassing rates of CO_2 were 3.3 mmol m^{-2} h^{-1}. By contrast, the CH_4 (11.7 μmol m^{-2} h^{-1}) and N_2O (2.8 μmol m^{-2} h^{-1}) emissions had only minor roles (Table S1). After converting the diffusive CO_2, CH_4 and N_2O fluxes to CO_2-equivalent emissions, the average emission of 146 mg CO_2-equivalent m^{-2} h^{-1} for CO_2 was four times higher than that for N_2O (32 mg CO_2-equivalent m^{-2} h^{-1}) and the CH_4 emissions (5 mg CO_2-equivalent m^{-2} h^{-1}) were negligible (Fig. 5). The emissions of CO_2 were 1.5 times higher during the wet seasons (spring and summer) than the dry seasons ($n = 84$; $p < 0.05$). The mean seasonal fluxes of CH_4 and N_2O ($p > 0.05$) showed no significant difference.

Discussion

Tidal driven carbon export and seasonality

Although there were clear seasonal differences in the concentration of dissolved carbon in the estuary, our results showed that the mangroves acted as a source of DIC, TA and DOC to the estuary. The fact that the concentrations of DIC and DOC were both higher in the tidal creek during the ebb tide than in the estuary suggests a net export from the mangrove forest to the estuary (Fig. 2). The high carbon values (Fig. 3) in the creek and large contribution of the mangrove forest to the estuary were both recorded during high-amplitude tides (Fig. 4). The tidal range determines the magnitude of tidal pumping and the positive correlations between the average offsets of DIC, TA, DOC and the tidal range (Fig. 4) confirmed the importance of groundwater seepage and tidal pumping in the lateral carbon export.

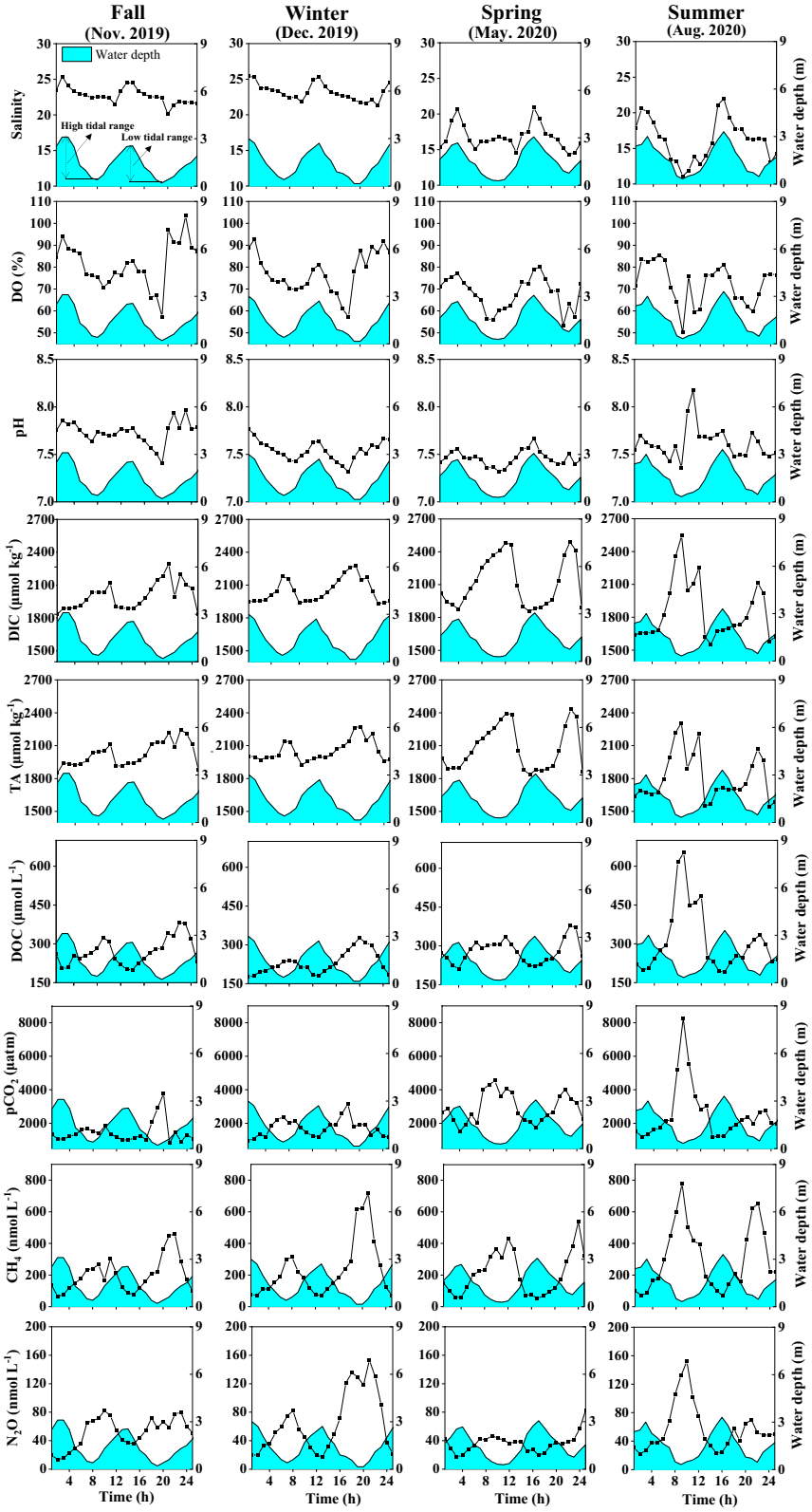

Fig. 3 Time series observations of salinity, DO, pH, DIC, TA, DOC, pCO_2, CH_4 and N_2O in the tidal creek in different seasons

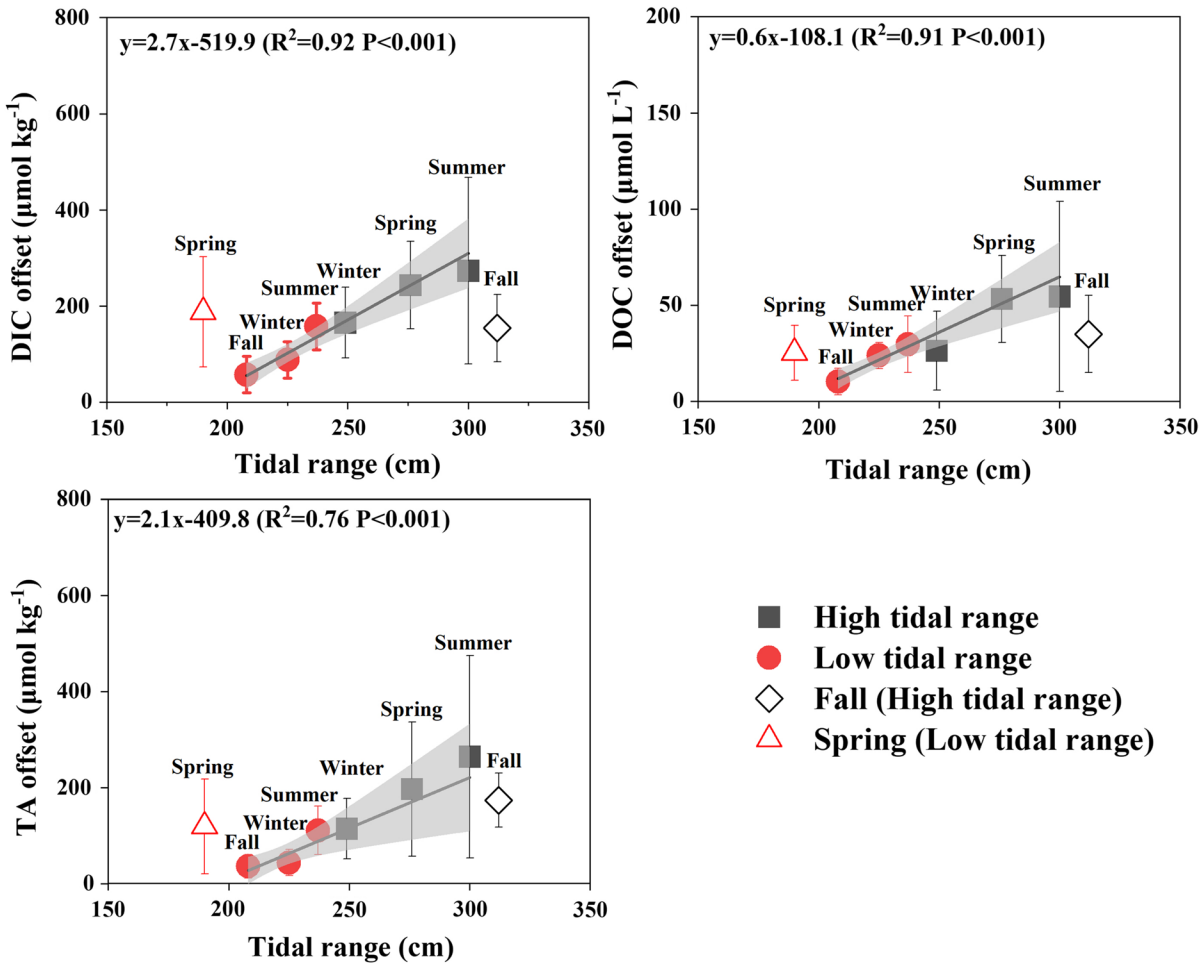

Fig. 4 Relationship between tidal range and carbon average offset in ebb tide from mixing line of estuary

The tidal range and porewater are considered to be the primary driving forces of the outwelling of nutrients and organic matter from mangrove forests (Dittmar and Lara 2001). DO followed a tidal cycle rather than a diurnal cycle, indicating that mixing processes were the main driver of DO rather than diurnal cycles of photosynthesis and respiration. DO and pH were low in the porewaters in the mangrove forest as a result of anaerobic conditions in the sediments (Alongi et al. 2005). The decreased DO and pH (Fig. 3) suggest the discharge of porewater into the tidal creek during ebb tides. As one of the most carbon-rich biomes, there are various mineralization processes in mangrove sediments that produce DIC and TA in porewater (Alongi 2014). The DOC in mangrove tidal creeks is mostly derived from the products of leachable organic matter in the mangrove sediments and root exudates (Kristensen et al. 2008b). Porewaters with a high concentration of solutes (DIC/DOC/TA) can be exported during the tidal cycle. The tidal range was an important variable affecting the export of porewater. On the one hand, tidal range controls the volume of water and the area of water–sediment contact. On the other hand, it also controls the vertical extent and period of porewater discharge based on hydraulic advection during ebb tides (Taillardat et al. 2018). The influence of the tidal range on solutes in porewaters was particularly obvious during low tides. The solute concentration in surface waters was higher during the period with a high tidal range than during the period with a low tidal range throughout the 25-h time series (asymmetrical

Table 1 Summary of time series observations (average ± SD) of water quality parameters and concentrations of DIC, TA, DOC and GHGs

Parameters	Units	Fall	Winter	Spring	Summer	Overall average
Rainfall	mm month^{-1}	0.2	21.1	70.5	172.5	66.1
Salinity		23.0 ± 1.1^{a}	23.5 ± 1.2^{a}	17.8 ± 1.9^{b}	15.3 ± 3.0^{b}	19.8 ± 3.2
Temperature	°C	21.2 ± 1.7^{a}	19.9 ± 1.1^{b}	25.8 ± 0.6^{c}	29.9 ± 0.8^{d}	24.2 ± 4.6
pH		7.75 ± 0.1^{a}	7.57 ± 0.1^{b}	7.48 ± 0.1^{c}	7.64 ± 0.2^{b}	7.47 ± 0.1
DO	% sat	83.4 ± 8.6^{a}	77.5 ± 9.4^{ab}	70.9 ± 6.8^{b}	72.8 ± 9.1^{c}	76.4 ± 3.9
DIC	μmol kg^{-1}	1958.3 ± 106.5^{a}	2002.2 ± 72.6^{a}	2013.8 ± 163.1^{a}	1713.5 ± 129.5^{b}	1893.3 ± 142.8
TA	μmol kg^{-1}	1995.8 ± 111.4^{a}	2011.5 ± 63.8^{a}	1983.2 ± 148.6^{a}	1701.5 ± 122.5^{b}	1897.5 ± 140.0
DOC	μmol L^{-1}	258.1 ± 55.4^{a}	214.3 ± 32.9^{b}	264.2 ± 41.9^{a}	249.5 ± 47.8^{a}	243.8 ± 21.1
pCO_2	μatm	1235.2 ± 235.4^{c}	1533 ± 423.4^{c}	2490.3 ± 636.8^{a}	1858.6 ± 540.2^{b}	1732.8 ± 604.7
CH_4	nmol L^{-1}	166.8 ± 99.2^{a}	152.8 ± 88.5^{a}	160.4 ± 123.6 ^{a}	204.8 ± 125.6 ^{a}	174.1 ± 23.1
N_2O	nmol L^{-1}	46.0 ± 22.3 ^{a}	49.1 ± 33.9 ^{a}	35.2 ± 15.1 ^{a}	41.1 ± 13.5 ^{a}	43.6 ± 6.8
Seepage water						
DIC	μmol kg^{-1}	4639.9	–	–	4862.6	–
TA	μmol kg^{-1}	3929.7	–	–	3656.9	–
DOC	μmol L^{-1}	383.7	–	–	488.6	–
pCO_2	μatm	25,880.9	–	–	36,490.3	–
CH_4	nmol L^{-1}	1916.1	–	–	425.5	–
N_2O	nmol L^{-1}	27.8	–	–	24.5	–

The data affected by sewage discharge are not included. Different letters (a, b, c) indicate statistical differences

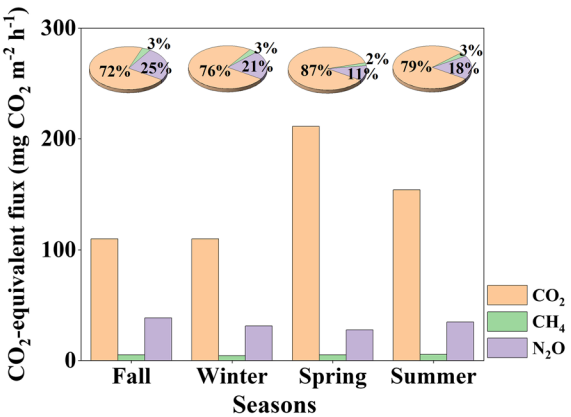

Fig. 5 CO_2-equivalent fluxes of greenhouse gases in different seasons. The pie charts represented the proportion of different gas fluxes

tide). This was mainly caused by greater hydraulic gradient due to higher tidal range, which drove more porewater export or groundwater discharge (Wilson and Gardner 2006; Xiao et al. 2017). Besides, the porewaters had a longer interactive time with the sediments during the period with a high tidal range. As a result, higher concentrations of solutes in porewater were discharged in to tidal creeks. A previous study also suggested that porewaters with higher concentrations of dissolved carbon from deeper layers are only exported during higher tidal range cycles (Marchand et al. 2004).

Rates of biogeochemical processes change with the season, resulting in variations in carbon concentrations and carbon export. In spring, even though the tide range was small, it still had a large offset value. By contrast, the tidal range was high in the fall, but the average offset value was small (Fig. 4). This implies that the season also affects the export of carbon from the tidal creek to the estuary. The effect of seasonal factors on the output of carbon from the mangrove creek to the estuary was reflected in two ways. First, higher temperatures accelerate the mineralization of organic carbon in mangrove wetlands, resulting in the increased production of DIC by accelerating the respiration of microorganisms and the activation energy (Fierer et al. 2006). Second, the concentration of DIC and TA in estuaries is reduced by the input of freshwater during the rainy seasons, especially in summer (Fig. 2). The average offset values were therefore high

during the low tidal range in spring. By contrast, the input of freshwater increases the DOC in estuaries during wet seasons. The contribution of DOC from the tidal creeks to the estuaries was therefore mainly determined by the contribution of the mangrove wetlands. The input of freshwater rich in nutrients may also affect the changes in electron acceptors required for the mineralization of organic matter, influencing the production of DIC and the consumption of DOC (Kristensen et al. 2008a). Our time series measurements of dissolved carbon confirmed that tidal range and seasonality were important factors in the regulation of the export of carbon from the mangrove creek to the estuary.

GHGs outgassing

The oversaturated concentrations of pCO_2, CH_4 and N_2O observed in the surface waters during the four series of observations suggested that the water surrounding the mangroves was a potential source of GHGs to the atmosphere. We found that there was no obvious seasonal variation in the CH_4 and N_2O dynamics, with similar gas concentrations and emissions produced in different seasons. The variability of CH_4 and N_2O was much higher on the tidal timescale than on the seasonal timescale. By contrast, the CO_2 dynamics showed significant seasonal variations. The CO_2 concentration and fluxes were higher in the wet seasons than in the dry seasons. This is consistent with previous research, which showed that the higher discharge of groundwater contributed to the high pCO_2 in wet seasons (Sadat-Noori et al. 2015). The input of organic carbon from the estuary to the wetlands was increased in the wet seasons and the temperatures were higher, which increased the mineralization of sediments, resulting in a higher production of CO_2 (Linto et al. 2014). During the ebb tide, porewaters rich in CO_2 flow into the tidal creek under the action of tidal pumping, which affects CO_2 concentrations in surface waters and the emission of CO_2 at the water–air interface (Call et al. 2015).

Many methods have been used to calculate the gas transfer velocity, resulting in a wide range of potential estimates (Chen et al. 2013). We calculated the flux of GHGs using three different gas transfer velocity models to illustrate the possible range (Table S1). The flux of GHGs calculated by method B04 was significantly higher (~50%) than that calculated by method R17. By contrast, the flux of GHGs calculated by method H16 was generally lower than that calculated by method R17. The Yunxiao mangrove creek is characterized by a strong current, low wind speeds and shallow water (<4 m). These characteristics are similar to the application environment of method R17 and therefore this model should give the most accurate estimate of the emission of GHGs from this mangrove site.

Because different GHGs have different global warming potentials, we converted the GHG emissions into CO_2-equivalents. On a global scale, CO_2, CH_4 and N_2O contribute 63, 11 and 6%, respectively, of the greenhouse effect (IPCC 2021). However, in our study area, N_2O made second highest the contribution to the total CO_2-equivalent greenhouse gas flux and CH_4 made the lowest contribution (Fig. 5). The magnitudes of the CO_2 and CH_4 emissions in our tidal creek were similar to those in other regions (Table 2). Interestingly, the emission of N_2O in our study area was significantly higher than that of other mangroves (Table 2). In pristine mangroves, the mangrove waters are a net N_2O sink. However, our results show that the tidal creek of this estuarine mangrove wetland is a hotspot for N_2O emissions.

Coupled biogeochemical processes regulating carbon export and GHGs emission

The biogeochemical processes in mangrove sediments are complex and the TA, DIC and GHGs concentrations are driven by redox reactions coupled to the mineralization of organic matter (Burdige 2011). The relationship between the salinity-normalized TA and DIC is useful in inferring the biogeochemical drivers of these parameters because they are directly affected by aerobic mineralization, sulfate reduction, denitrification and the dissolution of calcium carbonate (Bouillon et al. 2007).

There have only been a few observations of TA and DIC in mangrove creeks. The ratio of the salinity-normalized total alkalinity to the salinity-normalized DIC ranges from 0.54 to 0.92 (Fig. 6), similar to the slopes expected for a combination of aerobic respiration (−0.2), denitrification (0.9) and sulfate reduction (1.0). The driving factors are different in different study areas. For instance, the reduction of iron has been reported as the predominant degradation process for diagenetic carbon in the

Table 2 Comparison with literature data for CO_2, CH_4 and N_2O emission fluxes from surrounding waters in mangrove ecosystems

Country	Location	CO_2 emissions (mmol m^{-2} h^{-1})	CH_4 emissions (μmol m^{-2} h^{-1})	N_2O emissions (μmol m^{-2} h^{-1})	References
Australia	Darwin	1.7	na	−0.004	Maher et al. (2016)
Australia	Newcastle	1.9	na	0.03	Maher et al. (2016)
Australia	Barwon Heads	0.36	na	−0.04	Maher et al. (2016)
Australia	Korogoro Creek	36.2	1083	na	Sadat-Noori et al. (2016)
Australia	Moreton Bay	0.96 ± 1.75	1.37 ± 2.25	na	Call et al. (2015)
Australia	Evans Head	2.62 ± 6.9	11.25 ± 1.3	na	Santos et al. (2019)
New Caledonia	La For Estuary	3.3	na	na	Leopold et al. (2017)
India	Adyar Mangrove	2.02	216.6	na	Ramesh et al. (2007)
India	Sundarbans	4.7	0.83–5.8	na	Biswas et al. (2007) and Dutta et al. (2019)
Tanzania	Mtoni	0.13–1.7	2.91–14.58	na	Kristensen et al. (2008b)
Vietnam	Main Channel	1.1–3.4	na	na	Kone and Borges (2008)
Vietnam	Tam Giang	5.4–5.9	na	na	Kone and Borges (2008)
USA	Shark River	7.75	20	na	Rosentreter et al. (2017)
USA	Florida Bay	0.19	na	na	Millero et al. (2001)
Bermuda	Mangrove Bay	2.7	na	na	Zablocki et al. (2011)
Andaman	Wright	na	12–33	0.1–1.3	Barnes et al. (2006)
Puerto Rico	Magueyees	na	na	0.05–1.4	Bauza et al. (2002)
Kenya	Kinondo Creek	3.0	na	na	Bouillon et al. (2007)
Madagascar	Betsiboka	0.38	na	na	Ralison et al. (2008)
Brazil	Itacuraca Creek	4.7	na	na	Borges et al. (2003)
Papua New Guinea	Nagada	1.8	na	na	Borges et al. (2003)
China	Yunxiao Creek	2.4–4.8	10.8–19.5	1.3–4.0	This study

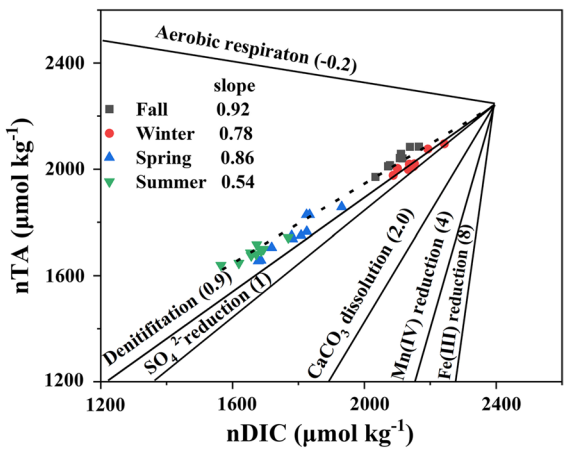

Fig. 6 Scatter plot between salinity-normalized TA and DIC concentrations during the ebb tides. The salinity normalization followed the method developed by Bouillon et al (2007). The dotted lines indicated linear fitting of all data

Bangrong mangroves of Thailand (Kristensen et al. 2000), whereas manganese reduction and denitrification–nitrification coupled with aerobic respiration accounted for most of the degradation of organic matter in the Matang mangroves of Malaysia (Alongi 1998). In general, aerobic respiration and sulfate reduction are the main processes in the degradation of organic matter in mangrove sediments (Kone and Borges 2008). Denitrification is assumed to be a minor mineralization pathway in pristine mangrove sediments (Kone and Borges 2008) with low nitrate concentrations ranging from below the limit of detection to 1 μmol L^{-1} (Maher et al. 2016). In these areas, Maher et al. (2016) found that creek waters were a net N_2O sink for the atmosphere (Table 2). This result is significantly different from our estuarine mangrove wetland with high input of riverine nitrogen. Our study area has a high concentration of dissolved N_2O (50.9 nmol L^{-1}) compared with pristine mangrove wetlands (6.5 nmol L^{-1}) (Maher et al. 2016). Tidal

waters from the estuary have high NO_3-N concentrations (> 140 μmol L^{-1}), which infiltrate the sediments and undergo complex biogeochemical processes, such as denitrification and the dissimilatory reduction of nitrate to the ammonium ion (Wang et al. 2019). More importantly, our previous study identified that incomplete denitrification in sediments in this study area is an important source of N_2O and that the majority of dissolved N_2O is transported to the tidal creek (Wang et al. 2019). The CO_2 produced by the mineralization process coupled with denitrification accounts for 51% of the total carbon dioxide production (Supplemental information, text S2). This also proved that denitrification plays an important role in the mineralization process of organic matter and greenhouse gas emissions. Denitrification is therefore one of the key processes driving the TA and production of DIC. We speculate that the infiltration of estuarine water with high levels of NO_3-N into the sediments will not only increase the discharge of N_2O from the sediments, but also increase the lateral TA and DIC export. This may not be conducive to the burial of carbon in sediments.

Mangrove forests are very efficient consumers of dissolved nitrogen from tidal water as a result of the rapid adsorption of nitrogen by the mangrove and transformation by soil microorganisms (Alongi 2020b; Reis et al. 2017). Seawater rich in nitrate and nitrite enters the mangrove sediments under the influence of tides. Some of the dissolved inorganic nitrogen is absorbed by plants and some is used by microorganisms. By restoring mangroves and controlling the anthropogenic loading of nitrogen in estuaries, we can accelerate the utilization of inorganic nitrogen by mangroves while reducing denitrification, which will help to reduce N_2O emissions and increase the accumulation of organic carbon by sediments.

Conclusions

Through the observations of times series in different seasons, this study identified that the lateral dissolved carbon export is regulated by both the tidal range and season. We focused on the emission of GHGs (CO_2, CH_4 and N_2O) at the water–air interface. The mangrove acted as a net source of TA, DIC, DOC and GHGs. To compare the effects of different GHGs, we converted CH_4 and N_2O into CO_2-equivalents. The CO_2-equivalent greenhouse gas fluxes are ranked as $CO_2 > N_2O > CH_4$. Unlike the creek waters of pristine mangroves, which are a sink for N_2O, our study area was affected by nitrogen-associated eutrophication and was a net source of N_2O. Based on the emissions of N_2O and the stoichiometric relationship between the TA and DIC, we suggest that denitrification is an important coupled remineralization process in organic matter. These biogeochemical processes may not be conducive to the burial of blue carbon in mangrove sediments. We suggest that it is crucial to account for the lateral dissolved carbon export and the flux of GHGs when evaluating the potential of mangroves as a sink for carbon, especially in an estuarine mangrove wetland with high input of riverine nitrogen.

Acknowledgements This research was supported by the Key Laboratory of the Coastal and Wetland Ecosystems, and the state Key Laboratory of Marine Environmental Science. We thank Zetao Wu, Mingzhen Zhang for assistance in fieldwork. We thank Xudong Zhu for providing wind speed data recorded by an eddy covariance tower in study site. Special thanks are given to faculty members from the Administrative Bureau of the Zhangjiang Estuary Mangrove National Nature Reserve, Yunxiao, for their support in the research. We are grateful to the editor and two anonymous reviewers for their thoughtful comments.

Author contributions LZ, WF and CN led the experimental design and approach. LZ, XK, WF, WY and YQ completed with sample collection and data analysis. CP contributed hydrologic data. LZ drafted the manuscript. XK and CN assisted with review and manuscript editing.

Funding This research was funded by the National Natural Science Foundation of China (Grant Nos. 42276171, 41976138, 41907162).

Data availability The datasets generated during the current study will be available from the corresponding author on reasonable request.

Declarations

Competing interests The authors declare that they have no conflict of interest.

Ethical approval Not applicable.

References

Adam P (2011) The energetics of mangrove forests. Aust J Ecol 36:E18–E19. https://doi.org/10.1111/j.1442-9993.2010.02190.x

Alongi DM (1998) Coastal ecosystem processes. CRC Press, Boca Raton

Alongi DM (2014) Carbon cycling and storage in mangrove forests. Annu Rev Mar Sci. https://doi.org/10.1146/annurev-marine-010213-135020

Alongi DM (2020a) Carbon cycling in the world's mangrove ecosystems revisited: significance of non-steady state diagenesis and subsurface linkages between the forest floor and the coastal ocean. Forests 11:977. https://doi.org/10.3390/fl1090977

Alongi DM (2020b) Nitrogen cycling and mass balance in the world's mangrove forests. Nitrogen 1:167–189. https://doi.org/10.3390/nitrogen1020014

Alongi DM, Pfitzner J, Trott LA et al (2005) Rapid sediment accumulation and microbial mineralization in forests of the mangrove *Kandelia candel* in the Jiulongjiang Estuary, China. Estuar Coast Shelf Sci 63:605–618. https://doi.org/10.1016/j.ecss.2005.01.004

Atwood TB, Connolly RM, Almahasheer H et al (2017) Global patterns in mangrove soil carbon stocks and losses. Nat Clim Change 7:523–528. https://doi.org/10.1038/nclimate3326

Barnes J, Ramesh R, Purvaja R et al (2006) Tidal dynamics and rainfall control N_2O and CH_4 emissions from a pristine mangrove creek. Geophys Res Lett 33:161–177. https://doi.org/10.1029/2006gl026829

Bauza JF, Morell JM, Corredor JE (2002) Biogeochemistry of nitrous oxide production in the red mangrove (*Rhizophora mangle*) forest sediments. Estuar Coast Shelf Sci 55:697–704. https://doi.org/10.1006/ecss.2001.0913

Biswas H, Mukhopadhyay SK, Sen S et al (2007) Spatial and temporal patterns of methane dynamics in the tropical mangrove dominated estuary, NE coast of Bay of Bengal, India. J Mar Syst 68:55–64. https://doi.org/10.1016/j.jmarsys.2006.11.001

Borges A, Djenidi S, Lacroix G et al (2003) Atmospheric CO_2 flux from mangrove surrounding waters. Geophys Res Lett. https://doi.org/10.1029/2003gl017143

Borges AV, Vanderborght JP, Schiettecatte LS et al (2004) Variability of the gas transfer velocity of CO_2 in a macrotidal estuary (the Scheldt). Estuaries 27:593–603. https://doi.org/10.1007/bf02907647

Bouillon S, Dehairs F, Velimirov B et al (2007) Dynamics of organic and inorganic carbon across contiguous mangrove and seagrass systems (Gazi Bay, Kenya). J Geophys Res 112:1–14. https://doi.org/10.1029/2006JG000325

Bouillon S, Borges AV, Castaneda-Moya E et al (2008) Mangrove production and carbon sinks: a revision of global budget estimates. Glob Biogeochem Cycles 22:1–12. https://doi.org/10.1029/2007gb003052

Breithaupt JL, Smoak JM, Smith TJ et al (2012) Organic carbon burial rates in mangrove sediments: strengthening the global budget. Glob Biogeochem Cycles 26:1–11. https://doi.org/10.1029/2012gb004375

Burdige DJ (2011) Estuarine and coastal sediments – coupled biogeochemical cycling. Treatise on Estuarine and Coastal Science, Academic Press, Waltham. https://doi.org/10.1016/B978-0-12-374711-2.00511-8

Cai WJ, Dai M, Wang Y et al (2004) The biogeochemistry of inorganic carbon and nutrients in the Pearl River estuary and the adjacent Northern South China Sea. Cont Shelf Res 24:1301–1319. https://doi.org/10.1016/j.csr.2004.04.005

Call M, Maher DT, Santos IR et al (2015) Spatial and temporal variability of carbon dioxide and methane fluxes over semi-diurnal and spring-neap-spring timescales in a mangrove creek. Geochim Cosmochim Acta 150:211–225. https://doi.org/10.1016/j.gca.2014.11.023

Chen C, Beardsley RC, Cowles GJO (2006) An unstructured grid, finite-volume coastal ocean model (FVCOM) system. Oceanography 19:78–89. https://doi.org/10.5670/oceanog.2006.92

Chen CTA, Huang TH, Chen YC et al (2013) Air-sea exchanges of CO_2 in the world's coastal seas. Biogeosciences 10:6509–6544. https://doi.org/10.5194/bg-10-6509-2013

Cole JJ, Caraco NF (2001) Emissions of nitrous oxide (N_2O) from a tidal, freshwater river, the Hudson River, New York. Environ Sci Technol 35:991–996. https://doi.org/10.1021/es0015848

Cotovicz LC Jr, Knoppers BA, Brandini N et al (2016) Spatio-temporal variability of methane (CH_4) concentrations and diffusive fluxes from a tropical coastal embayment surrounded by a large urban area (Guanabara Bay, Rio de Janeiro, Brazil). Limnol Oceanogr 61:S238–S252. https://doi.org/10.1002/lno.10298

Dittmar T, Lara RJ (2001) Driving forces behind nutrient and organic matter dynamics in a mangrove tidal creek in North Brazil. Estuar Coast Shelf Sci 52:249–259. https://doi.org/10.1006/ecss.2000.0743

Donato DC, Kauffman JB, Murdiyarso D et al (2011) Mangroves among the most carbon-rich forests in the tropics. Nat Geosci 4:293–297. https://doi.org/10.1038/ngeo1123

Fierer N, Colman BP, Schimel JP et al (2006) Predicting the temperature dependence of microbial respiration in soil: a continental-scale analysis. Glob Biogeochem Cycles 20:1–10. https://doi.org/10.1029/2005gb002644

Ho DT, Coffineau N, Hickman B et al (2016) Influence of current velocity and wind speed on air-water gas exchange in a mangrove estuary. Geophys Res Lett 43:3813–3821. https://doi.org/10.1002/2016gl068727

IPCC (2021) Summary for Policymakers. In: Climate Change 2021: The Physical Science Basis. Contribution of Working Group I to the Sixth Assessment Report of the Intergovernmental Panel on Climate Change. Cambridge University Press. https://doi.org/10.1017/9781009157896.009

Kelleway JJ, Saintilan N, Macreadie PI et al (2016) Sedimentary factors are key predictors of carbon storage in SE Australian saltmarshes. Ecosystems 19:865–880. https://doi.org/10.1007/s10021-016-9972-3

Kone YJM, Borges AV (2008) Dissolved inorganic carbon dynamics in the waters surrounding forested mangroves of the Ca Mau Province (Vietnam). Estuar Coast Shelf Sci 77:409–421. https://doi.org/10.1016/j.ecss.2007.10.001

Kristensen E, Andersen FO, Holmboe N et al (2000) Carbon and nitrogen mineralization in sediments of the Bangrong mangrove area, Phuket, Thailand. Aquat Microb Ecol 22:199–213. https://doi.org/10.3354/ame022199

Kristensen E, Bouillon S, Dittmar T et al (2008a) Organic carbon dynamics in mangrove ecosystems: a review. Aquat Bot 89:201–219. https://doi.org/10.1016/j.aquabot.2007.12.005

Kristensen E, Flindt MR, Ulomi S et al (2008b) Emission of CO_2 and CH_4 to the atmosphere by sediments and open waters in two Tanzanian mangrove forests. Mar Ecol-Prog Ser 370:53–67. https://doi.org/10.3354/meps07642

Leopold A, Marchand C, Deborde J et al (2017) Water biogeochemistry of a mangrove-dominated estuary under a semi-arid climate (New Caledonia). Estuaries Coasts 40:773–791. https://doi.org/10.1007/s12237-016-0179-9

Lewis E, Wallace D, Allison LJ (1998) Program developed for CO_2 system calculations

Linto N, Barnes J, Ramachandran R et al (2014) carbon dioxide and methane emissions from mangrove-associated waters of the andaman islands, bay of bengal. Estuaries Coasts 37:381–398. https://doi.org/10.1007/s12237-013-9674-4

Livesley SJ, Andrusiak SM (2012) Temperate mangrove and salt marsh sediments are a small methane and nitrous oxide source but important carbon store. Estuar Coast Shelf Sci 97:19–27. https://doi.org/10.1016/j.ecss.2011.11.002

Lovelock CE, Feller IC, Reef R et al (2014) Variable effects of nutrient enrichment on soil respiration in mangrove forests. Plant Soil 379:135–148. https://doi.org/10.1007/s11104-014-2036-6

Luo M, Zhu WF, Huang JF et al (2019) Anaerobic organic carbon mineralization in tidal wetlands along a low-level salinity gradient of a subtropical estuary: rates, pathways, and controls. Geoderma 337:1245–1257. https://doi.org/10.1016/j.geoderma.2018.07.030

Maher DT, Santos IR, Golsby-Smith L et al (2013) Groundwater-derived dissolved inorganic and organic carbon exports from a mangrove tidal creek: the missing mangrove carbon sink? Limnol Oceanogr 58:475–488. https://doi.org/10.4319/lo.2013.58.2.0475

Maher DT, Sippo JZ, Tait DR et al (2016) Pristine mangrove creek waters are a sink of nitrous oxide. Sci Rep 6:1–8. https://doi.org/10.1038/srep25701

Maher DT, Call M, Santos IR et al (2018) Beyond burial: lateral exchange is a significant atmospheric carbon sink in mangrove forests. Biol Lett 14:1–4. https://doi.org/10.1098/rsbl.2018.0200

Marchand C, Baltzer F, Lallier-Verges E et al (2004) Porewater chemistry in mangrove sediments: relationship with species composition and developmental stages (French Guiana). Mar Geol 208:361–381. https://doi.org/10.1016/j.margeo.2004.04.015

Mazda Y, Ikeda Y (2006) Behavior of the groundwater in a riverine-type mangrove forest. Wetl Ecol Manag 14:477–488. https://doi.org/10.1007/s11273-006-9000-z

Millero FJ, Hiscock WT, Huang F et al (2001) Seasonal variation of the carbonate system in Florida Bay. Bull Mar Sci 68:101–123

Ralison OH, Borges AV, Dehairs F et al (2008) Carbon biogeochemistry of the Betsiboka estuary (north-western Madagascar). Org Geochem 39:1649–1658. https://doi.org/10.1016/j.orggeochem.2008.01.010

Ramesh R, Purvaja R, Neetha V et al (2007) CO_2 and CH_4 emissions from Indian mangroves and surrounding waters. In: Tateda Y, Upstill-Goddard R, Goreau T, Alongi D, Nose A, Kristensen E, Wattayakorn G (eds) Greenhouse gas and carbon balances in mangrove coastal ecosystems. Maruzen Publishing, Kanagawa

Reis CRG, Nardoto GB, Oliveira RS (2017) Global overview on nitrogen dynamics in mangroves and consequences of increasing nitrogen availability for these systems. Plant Soil 410:1–19. https://doi.org/10.1007/s11104-016-3123-7

Reithmaier GMS, Ho DT, Johnston SG et al (2020) Mangroves as a source of greenhouse gases to the atmosphere and alkalinity and dissolved carbon to the coastal ocean: a case study from the Everglades National Park, Florida. J Geophys Res 125:1–16. https://doi.org/10.1029/2020jg005812

Rosentreter JA, Maher DT, Ho DT et al (2017) Spatial and temporal variability of CO_2 and CH_4 gas transfer velocities and quantification of the CH_4 microbubble flux in mangrove dominated estuaries. Limnol Oceanogr 62:561–578. https://doi.org/10.1002/lno.10444

Sadat-Noori M, Santos IR, Sanders CJ et al (2015) Groundwater discharge into an estuary using spatially distributed radon time series and radium isotopes. J Hydrol 528:703–719. https://doi.org/10.1016/j.jhydrol.2015.06.056

Sadat-Noori M, Maher DT, Santos IR (2016) Groundwater discharge as a source of dissolved carbon and greenhouse gases in a subtropical estuary. Estuar Coasts 39:639–656. https://doi.org/10.1007/s12237-015-0042-4

Sanders CJ, Santos IR, Maher DT et al (2016) Examining $^{239+240}$pu, ^{210}Pb and historical events to determine carbon, nitrogen and phosphorus burial in mangrove sediments of Moreton Bay, Australia. J Environ Rasioactiv 151:623–629. https://doi.org/10.1016/j.jenvrad.2015.04.018

Santos IR, Eyre BD, Huettel M (2012) The driving forces of porewater and groundwater flow in permeable coastal sediments: a review. Estuar Coast Shelf Sci 98:1–15. https://doi.org/10.1016/j.ecss.2011.10.024

Santos IR, Maher DT, Larkin R et al (2019) Carbon outwelling and outgassing vs. burial in an estuarine tidal creek surrounded by mangrove and saltmarsh wetlands. Limnol Oceanogr 64:996–1013. https://doi.org/10.1002/lno.11090

Taillardat P, Ziegler AD, Friess DA et al (2018) Carbon dynamics and inconstant porewater input in a mangrove tidal creek over contrasting seasons and tidal amplitudes. Geochim Cosmochim Acta 237:32–48. https://doi.org/10.1016/j.gca.2018.06.012

Tait DR, Maher DT, Macklin PA et al (2016) Mangrove pore water exchange across a latitudinal gradient. Geophys Res Lett 43:3334–3341. https://doi.org/10.1002/2016gl068289

Taniguchi M, Burnett WC, Cable JE et al (2002) Investigation of submarine groundwater discharge. Hydrol Process 16:2115–2129. https://doi.org/10.1002/hyp.1145

Wang M, Zhang J, Tu Z et al (2010) Maintenance of estuarine water quality by mangroves occurs during flood periods: a case study of a subtropical mangrove wetland. Mar Pollut Bull 60:2154–2160. https://doi.org/10.1016/j.marpolbul.2010.07.025

Wang FF, Chen NW, Yan J et al (2019) Major processes shaping mangroves as inorganic nitrogen sources or sinks: insights from a multidisciplinary study. J Geophys Res-Biogeo 124:1194–1208. https://doi.org/10.1029/2018jg004875

Weiss RF (1974) Carbon dioxide in water and seawater: the solubility of a non-ideal gas. Mar Chem 2:203–215. https://doi.org/10.1016/0304-4203(74)90015-2

Wilson AM, Gardner LR (2006) Tidally driven groundwater flow and solute exchange in a marsh: numerical simulations. Water Resour Res. https://doi.org/10.1029/2005WR004302

Wu K, Dai M, Chen J et al (2015) Dissolved organic carbon in the South China Sea and its exchange with the Western Pacific Ocean. Deep Sea Res 122:41–51. https://doi.org/10.1016/j.dsr2.2015.06.013

Xiao K, Li H, Wilson AM et al (2017) Tidal groundwater flow and its ecological effects in a brackish marsh at the mouth of a large sub-tropical river. J Hydrol 555:198–212. https://doi.org/10.1016/j.jhydrol.2017.10.025

Yamamoto S, Alcauskas JB, Crozier TE (1976) Solubility of methane in distilled water and seawater. J Chem Eng Data 21:78–80. https://doi.org/10.1021/je60068a029

Zablocki JA, Andersson AJ, Bates NR (2011) Diel aquatic CO_2 system dynamics of a Bermudian mangrove environment. Aquat Geochem 17:841. https://doi.org/10.1007/s10498-011-9142-3

Zhang YH, Wang WQ, Cheng WQ et al (2006) The growth of Kandelia candel seedlings in mangrove habitats of the Zhangjiang estuary in Fujian, China. Acta Ecol Sin 26:1648–1655. https://doi.org/10.1016/S1872-2032(06)60028-0

Zhou HC, Wei SD, Zeng Q et al (2010) Nutrient and caloric dynamics in Avicennia marina leaves at different developmental and decay stages in Zhangjiang River Estuary, China. Estuar Coast Shelf Sci 87:21–26. https://doi.org/10.1016/j.ecss.2009.12.005